

# FABRICATION OF THE RFQ III FOR THE J-PARC LINAC CURRENT UPGRADE

T. Morishita<sup>#</sup>, Y. Kondo, H. Oguri, K. Hasegawa, JAEA, Tokai, Japan  
H. Kawamata, T. Sugimura, F. Naito, KEK, Tsukuba, Japan

## Abstract

The J-PARC linac has been in operation for users with a beam energy of 181 MeV. An upgrade of the energy (up to 400MeV) and current (up to 50mA) of the linac is scheduled for a 1MW operation at the Rapid-Cycling Synchrotron (RCS). For the current upgrade, the RFQ III, which is designed for 50mA beam acceleration, has been fabricated. The engineering design and the fabrication technologies were the same as those for the RFQ II in the J-PARC linac. Some engineering methods have been improved for dimensional accuracy, reliability, and fabrication time. In the RFQ III fabrication, a vane deformation along the longitudinal direction occurred after the finish machining. We reduced this deformation by changing the method of fixation in the assembly at the brazing. The fabrication of the cavity was completed and the field tuning was performed. The high-power conditioning and the beam acceleration tests are presently underway.

## INTRODUCTION

The J-PARC accelerator comprises an injector linac, a 3-GeV Rapid-Cycling Synchrotron (RCS) and a 50-GeV Main Ring. The J-PARC linear accelerator consists of an ion source, a radio-frequency quadrupole (RFQ) linac, drift tube linacs (DTLs), separated DTLs (SDTLs), and the beam transport line to the RCS [1].

The J-PARC linac has been operating for users with a beam energy of 181 MeV. The currently operating RFQ is a 4-vane type cavity that is used to accelerate a negative hydrogen beam from 50 keV to 3 MeV with a peak current of 30mA. The RF duty factor is 3% (600  $\mu$ s at 50 Hz). For quick replacement in case of trouble with the RFQ, we fabricated a spare RFQ (RFQII) as a backup machine. [2–4]

The upgrade to the energy (up to 400MeV) and current (up to 50mA) of the linac is scheduled for 1 MW operation at RCS. The beam dynamics of the RFQ are newly designed for the beam current upgrade to 50 mA operation [5–7]. The fabrication of the new RFQ (RFQ III) was completed in March 2013. The high-power conditioning started in this April.

## FABRICATION

Engineering design features of RFQ III are listed in Table 1. The cavity is divided into three unit tanks. The tanks (about 1.2 m long each) are integrated on a single platform. The vanes were machined by numerical-controlled machining using end mills, and chemically polished to obtain a smooth surface before brazing. Figure 1 is the unit 3 (downstream) tank after the brazing. Ports

for the tuner, cooling water, and plugging of the drilled-through holes are also brazed simultaneously with the vanes.

Table 1: Engineering Design Features

Material	High-purity oxygen-free copper with Hot Isostatic Pressing (HIP)
Annealing after roughing	About 1 mm margin for finishing. 600 degree C in vacuum furnace.
Finish machining	Numerical-controlled machining with end-mills
Surface treatment	Chemical polishing (3–5 $\mu$ m), Chromating
Integration method	Vanes and ports are joined by brazing

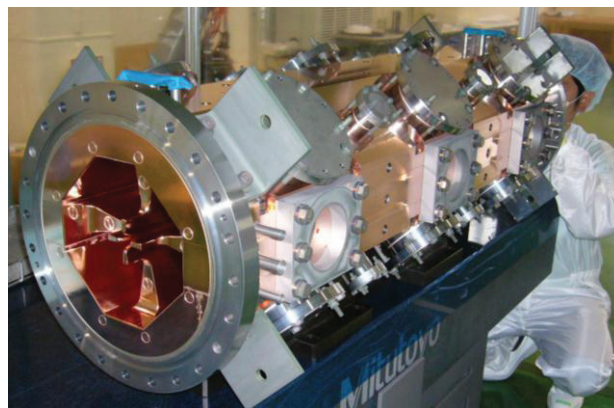


Figure 1: Unit 3 (downstream) tank after brazing.

## Vane Deformation after Finish Machining

The tank is formed by brazing the major and minor vanes. After the finish machining, the dimensional and geometric errors were less than 0.03 mm confirmed by a coordinate measuring machine (CMM) before surface treatment. However, at the assembly process prior to brazing, the geometric error (warpage of about 0.10–0.13 mm for a 1.2 m vane as shown in Fig. 2) was found for both major and minor vanes of unit 1 and 2 tanks. The fabrication process after the finishing was the surface treatment. At first, we suspected that the thermal stress of the hot bath degreasing in the surface treatment process was the cause. However, there was no deformation by the thermal stress test. Next, we suspected the residual strain from the finish machining. The inner surfaces were machined by ball-end and corner-R-end mills, and the outer surfaces were machined by face mills, details of

<sup>#</sup>takatoshi.morishita@j-parc.jp

which are described in Ref. [3]. The difference between these cutting conditions might induce an imbalance in the residual strain. In the fabrication of the unit 1 and 2 tanks, vanes were assembled 3 months after the finishing. The residual strain might deform the vane gradually during this period.

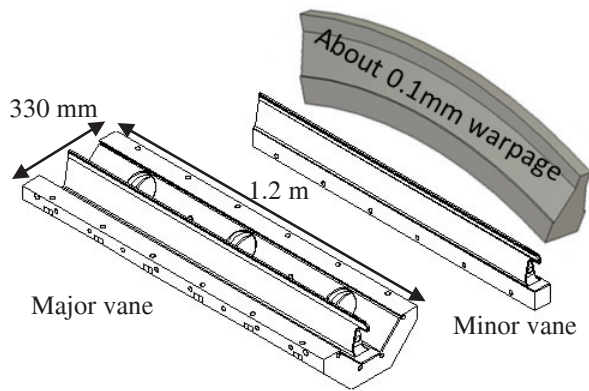


Figure 2: Schematic drawings of the vanes. The width of the major vane is 330mm. The geometric deformation of the major vane is the same direction. The deformation in the orthogonal direction did not appear in both vanes.

To reduce this geometric error, the minor vane was corrected by adding stainless steel plates to the side walls of the major vanes in assembly. Major vanes were corrected by bolting them together in the head-on position. Figure 3 shows the assembly for brazing. After brazing, the deformation by above mentioned warpage was reduced to 0.03 mm.

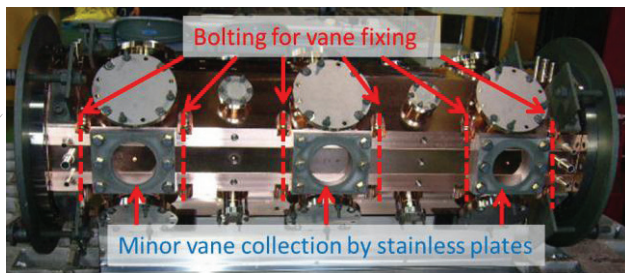


Figure 3: Assembly for brazing.

Fabrication procedures for the vanes for the unit 3 tank were the same as units 1 and 2. However, those were assembled and brazed quickly after the finish machining. Warpage did not appear in the unit 3 tank, and the deformation by the brazing was within 0.01 mm.

### Position Accuracy after Brazing

After the brazing, a dimension of the unit cavity was measured. Figure 4 shows the relative position errors between vane tips at both ends of the unit tanks and outer width of the cavities. For units 1 and 2, these were outward deformations of about 0.03 mm. Besides, the cavity width is close to the design value at the longitudinal center of the cavity; therefore, the dimension error occurred like the flared horn shape for units 1 and 2 due to the vane deformation. In the unit 3 tank, such

deformation did not appear. Meanwhile, there can be seen a twisted deformation of about 0.03 mm between the upstream and downstream ends.

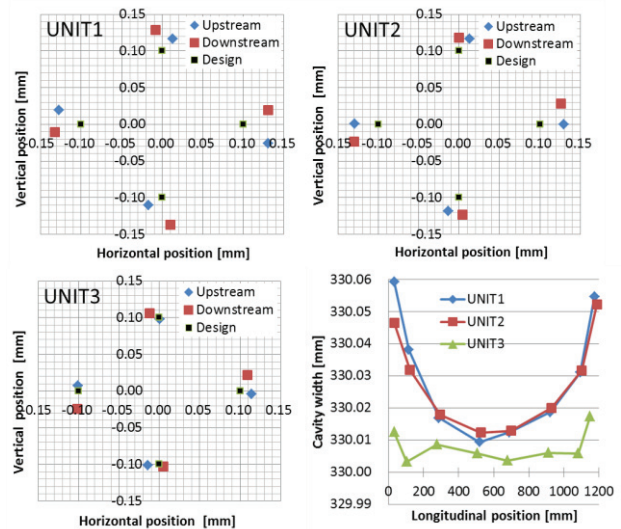


Figure 4: Relative position error between vane tips at both ends of the unit tanks and outer width of the cavity.

## LOW-LEVEL TUNING

After brazing, the units were integrated on the platform. The movable tuners, the endplates, and the loop coupler were installed for low-level tuning. The drive units were attached for the bead-perturbation measurement at each end of the platform. Figure 5 shows the setup of this measurement.

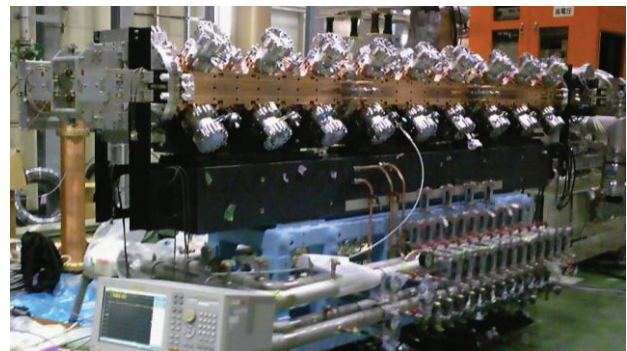


Figure 5: Setup of the bead-perturbation measurement.

Knobs for the low-level tuning are as follows:

- Heights of the tuners and the loop coupler for frequency and field uniformity.
- Heights of the dipole stabilizing rods for dipole mode separation.
- Rotational angle of the loop coupler for input RF coupling.

The field tuning procedures are as follows:

- Dipole rods are inserted for centering the operating mode between dipole modes
- Tuners are moved for flattening the field strength longitudinally, and balancing between quadrants. The

response of each tuner was measured to determine the positioning of the tuners calculated by the pseudo-inverse matrix method.

- All tuners are moved to adjust the frequency.

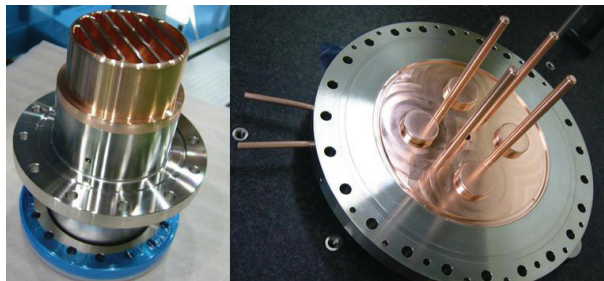


Figure 6: High-power tuner and endplate. Oxygen-free copper and stainless steel flange are brazed. Tuner has slits for vacuum pumping.

The tuning procedures were iterated and the dimensions of the low-level parts were determined. Figure 6 shows the high-power tuner and the endplate. These high-power parts have a water cooling channel and are equipped with an RF contact. Figure 7 shows the distribution of the quadrupole component and dipole elements with high-power tuners and a high-power coupler. Uniformity of the quadrupole field is typically 1 %. The mixed dipole modes are less than 2 % of the quadrupole field. Table 2 shows the RF characteristics with high-power parts.

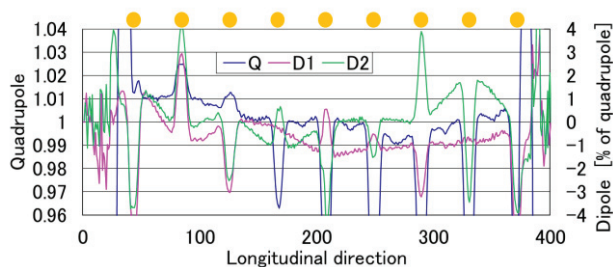


Figure 7: Longitudinal distribution of the quadrupole component and dipole elements.

Table 2: RF Characteristics of RFQ III

Parameter	Value	Note
Frequency at nominal water temperature [MHz]	324.013	Design : 324.000 Tuning range by water temperature control: +/- 0.15MHz
Nearest dipole mode frequency [MHz]	319.4	Operating mode locates between the 3 <sup>rd</sup> and 4 <sup>th</sup> dipole modes
Unloaded Q-value	10100	90% of the SUPERFISH calc.

## SETUP FOR THE BEAM ACCELERATION TEST

The RFQ III high-power test stand has been set up as shown in Fig. 8. We added three 400 L/s ion pumps and three 1700 (for N<sub>2</sub>) L/s cryogenic pumps to the RFQ. The vacuum pressure in the cavity is 6e-6 Pa before the high-power conditioning. The resonant frequency is tuned by controlling the water temperature through the vane by the chiller unit.

The high-power conditioning started at the end of April 2013. We will start the beam test in May 2013.

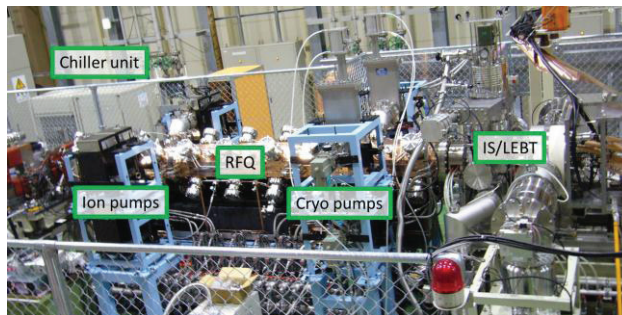


Figure 8: View of the beam accelerator test stand.

## ACKNOWLEDGMENT

The authors would like to thank Mr. Y. Iino and Mr. H. Hatanaka of TOYAMA Co., Ltd. for the mechanical design and fabrication of J-PARC RFQ III.

## REFERENCES

- [1] Y. Yamazaki (eds), "Accelerator Technical Design Report for J-PARC," JAERI-Tech 2003-044; KEK-Report 2002-13.
- [2] T. Morishita et al., "Fabrication of the New RFQ for the J-PARC Linac," Proc. of 2010 International Particle Accelerator Conference, Kyoto, Japan, p. 783 (2010).
- [3] T. Morishita et al., Procs. of LINAC2010, Tsukuba, Japan, p. 518 and p.521 (2010).
- [4] Y. Kondo et al., "High-power test and thermal characteristics of a new radio-frequency quadrupole cavity for the Japan Proton Accelerator Research Complex linac," Phys. Rev. Stab 16, 040102 (2013).
- [5] Y. Kondo et al., "Recent Progress of J-PARC RFQs," Procs. of LINAC 2012, Tel Aviv, Israel (2012).
- [6] T. Morishita et al., "Progress on RFQIII Fabrication in J-PARC Linac," Procs. of LINAC 2012, Tel Aviv, Israel (2012).
- [7] Y. Kondo et al., "On-machine non-contact dimension-measurement system with laser displacement sensor for vane-tip machining of RFQs," NIMA, 667, p. 5(2011).